



Original Paper

Insight into the evolution of refractory basic and neutral nitrogen compounds during residue hydrotreating process

Zhong-Huo Deng^{*}, Si-Yang Guo, Xin-Peng Nie, Xin-Heng Cai, Yan-Zi Jia, Wei Han, Li-Shun Dai

Sinopec Research Institute of Petroleum Processing Co. Ltd, Beijing, 100083, China



ARTICLE INFO

Article history:

Received 9 July 2024

Received in revised form

30 December 2024

Accepted 23 February 2025

Available online 25 February 2025

Edited by Min Li

Keywords:

Residual oils

Nitrogen compounds

Hydrodenitrogenation

Molecular structure

Reaction mechanism

ABSTRACT

A comprehensive insight into the evolution and molecular structure of basic and neutral nitrogen compounds during the residue hydrotreating (RHT) process was gained through ESI(+)/ESI(−) FT-ICR MS analysis of the feedstock and its hydrogenated samples, with hydrodenitrogenation (HDN) ratios of 15.9%–70.1%. This study revealed that carbazoles, characterized by a double bond equivalent (DBE) of 9–11, were the refractory neutral nitrogen compounds during the RHT process. Their recalcitrant nature was primarily due to their low aromaticity and high steric hindrance. Conversely, quinolines (DBEs 7 to 9) were the most abundant basic nitrogen compounds. Through a meticulous analysis of DBE evolution, we revealed the intricate reaction mechanisms of benzocarbazoles and dibenzocarbazoles in residual oil, highlighting the crucial role of quinolines as key intermediates in eliminating these compounds. Interestingly, nitrogen compounds with either low or high carbon numbers (for a given DBE) exhibited higher reactivity than those with medium carbon numbers, which can be attributed to the low steric hindrance resulting from short alkyl chains and more naphthenic-aromatic structures, respectively. After hydro-treatment, the molecular structures of the most refractory or abundant nitrogen compounds could consist of two main types: those with multiple naphthenic-aromatic rings and those with long side chains near the nitrogen atom. This research has revealed nitrogen compounds' evolutionary mechanisms and refractory nature, and the molecular structure of the most resistant or abundant basic and neutral nitrogen compounds, providing a deeper understanding of the HDN process and ultimately paving the way for the rational RHT catalyst design and process development.

© 2025 The Authors. Publishing services by Elsevier B.V. on behalf of KeAi Communications Co. Ltd. This is an open access article under the CC BY-NC-ND license (<http://creativecommons.org/licenses/by-nc-nd/4.0/>).

1. Introduction

Hydrodenitrogenation (HDN) is a critical reaction during the residual oil hydrotreating (RHT) process, as the nitrogenous impurities can significantly diminish the catalytic performance of the downstream fluid catalytic cracking process and contribute to NO_x emissions during fuel combustion (Ho et al., 1992; Li et al., 2019; Prado et al., 2017). However, nitrogen is one of the most difficult heteroatoms to remove from residual oils (Liu et al., 2016; Ovalles et al., 2013). Industrial RHT units typically achieve a HDN ratio of merely 40%–55%, compared to 80%–90% for hydrodesulfurization (Deng et al., 2022). The low reactivity of nitrogen compounds in residual oils can be attributed to at least three factors. Firstly, studies

on model compounds have revealed that, due to the high binding energy of the carbon-nitrogen double bonds, HDN generally involves a lengthy reaction pathway, including sequential saturation of the N-heterocycle (frequently including aromatic rings), ring opening, and denitrogenation, with hydrogenation or ring breaking being the rate-determining step (Abu and Smith, 2007; Adamski et al., 2004; Bachrach et al., 2016; Bello et al., 2021; Furimsky and Massoth, 2005; Laredo et al., 2004; Massoth and Kim, 2003; Nguyen et al., 2017; Prado et al., 2017; Prins et al., 1997, 2005, 2006; Szymańska et al., 2003). Secondly, the basic nitrogen compounds such as pyridine and its derivatives can neutralize the acid sites of the hydrotreating catalyst, leading to coke formation (Furimsky, 1999). In contrast, neutral nitrogen compounds such as pyrrole and its derivatives can be converted to basic ones such as amines during the HDN process (Bello et al., 2021; Furimsky and Massoth, 2005; Prins et al., 2006). Therefore, nitrogen acts as a self-inhibitor in the RHT process,

^{*} Corresponding author.

E-mail address: dengzh.ripp@sinopec.com (Z.-H. Deng).

causing the HDN ratio to typically decrease as the nitrogen content in the feedstock increases (Ovalles et al., 2013). Finally, the residual oils have a refractory nature, characterized by high molecular weight, asphaltene content, viscosity, and nitrogen content (Ancheyta et al., 2005; Marafi et al., 2019). Given these complexities, enhancing HDN efficiency during the RHT process remains a significant challenge in the refining industry.

Unlike the model compounds, the nitrogen compounds in residual oils are highly substituted by alkyl chains, which can greatly alter their reactivity and reaction pathways (Furimsky and Massoth, 2005; Nguyen et al., 2019). Thus, gaining a profound understanding of the physicochemical properties of the refractory basic and neutral nitrogen compounds in residual oils is crucial for enhancing HDN efficiency. Ultrahigh-resolution Fourier transform ion cyclotron resonance mass spectrometry (FT-ICR MS), either alone or in combination with pre-fractionation techniques like SARA, can offer molecular-level insights into petroleum samples (Cho et al., 2012; Liu et al., 2016, 2018; Ni et al., 2018; Zhao et al., 2021). Moreover, the employment of various ionization methods in combination with FT-ICR MS enables the selective identification of different compounds. For instance, atmospheric pressure photoionization (APPI) gives an overall perspective of species in heavy oils, given its capacity to ionize a wide variety of substances. Positive ion electrospray ionization (ESI(+)) is capable of identifying basic nitrogen compounds, ketones, sulfoxides, and porphyrins. In contrast, negative ion ESI (ESI(-)) can selectively identify neutral nitrogen compounds, acids, and phenols. When the focus is on polar species, particularly N-containing compounds, ESI(+) and ESI(-) are the preferred choices, as supported by previous studies (Ávila et al., 2012; Li et al., 2024; Purcell et al., 2007; Zhang et al., 2014). Utilizing these analytical methods, the transformation of basic and neutral nitrogen compounds, along with the molecular structure of refractory nitrogen compounds, have been characterized throughout various heavy oil hydrotreating processes, including vacuum gas oil (VGO) (Celis-Cornejo et al., 2018; Guillemant et al., 2020; Lai et al., 2020; Le Maître et al., 2019, 2020; Li et al., 2024; Mikhaylova et al., 2022), coking gas oil (CGO) (Mikhaylova et al., 2022; Nguyen et al., 2019; Zhang et al., 2020), deasphalted oil (DAO) (Zhang et al., 2013), residual oils (Li et al., 2021; Liu et al., 2016, 2017, 2018; Zhang et al., 2020), asphaltenes (Chacón-Patiño et al., 2015; Mierau et al., 2015; Pei et al., 2017; Purcell et al., 2010; Rogel and Witt, 2017; Zhu et al., 2022), and so on. With these investigations, some of the refractory natures of nitrogen compounds in heavy oils have been well discussed. For example, it is well accepted that the nitrogen compounds with high aromaticity and low carbon number have high reactivity (Guillemant et al., 2019; Lai et al., 2020; Le Maître et al., 2019, 2020; Liu et al., 2018; Mikhaylova et al., 2022; Zhang et al., 2013), the neutral nitrogen compounds are more refractory than the basic ones, and the most refractory neutral nitrogen compounds are carbazoles (Celis-Cornejo et al., 2018; Guillemant et al., 2019; Le Maître et al., 2020; Li et al., 2021, 2024; Mikhaylova et al., 2022; Nguyen et al., 2019).

However, it is crucial to acknowledge that there are inconsistencies in the comprehension of HDN chemistry across these works. For instance, the double bond equivalent (DBE) of the most refractory basic nitrogen compounds ranges from 6 to 9 during various hydrotreatments of VGOs and CGOs (Lai et al., 2020; Li et al., 2024; Mikhaylova et al., 2022; Nguyen et al., 2019). Although some research indicates that the reactivity of neutral nitrogen compounds is unrelated to carbon number (Celis-Cornejo et al., 2018; Liu et al., 2016), numerous studies have demonstrated that the most refractory nitrogen compounds are carbazoles with extended alkyl chains (Guillemant et al., 2019; Lai et al., 2020; Le Maître et al., 2019, 2020; Liu et al., 2018; Mikhaylova et al., 2022; Zhang et al., 2013). One study of the atmospheric residue hydrotreating process

concluded that the basic nitrogen compounds are more refractory than the neutral ones (Liu et al., 2018), while many other studies have come to the opposite conclusion (Celis-Cornejo et al., 2018; Guillemant et al., 2019; Le Maître et al., 2020; Li et al., 2021, 2024; Mikhaylova et al., 2022; Nguyen et al., 2019). These conflicting findings can be attributed, at least partially, to the limitations of FT-ICR MS analysis and the intricate nature of the HDN reaction mechanisms. In FT-ICR MS data analysis, compounds are frequently grouped based on DBE and carbon number (Mikhaylova et al., 2022; Nguyen et al., 2019), yet compounds with identical DBE and carbon number can encompass numerous isomers exhibiting significant reactivity variations. Consequently, it is plausible to hypothesize that the reactivity order of nitrogen compounds identified by DBE and carbon number may vary as a function of HDN depth. Furthermore, during the heavy oil hydrotreating processes, the DBE and/or carbon number of these nitrogen compounds may be altered by various reactions, including HDN, dehydrogenation, condensation, and hydrocracking (Furimsky and Massoth, 2005; Nguyen et al., 2019). Put simply, the pseudo-compounds categorized by DBE and carbon number can act as both reactants and products (Liu et al., 2016). Therefore, an ideal approach to investigate this phenomenon would include a variety of samples over a wide range of HDN depths. This would allow the evolution of refractory nitrogen compounds to be observed throughout the hydroprocessing of heavy oil. However, with rare exceptions (Liu et al., 2017, 2018; Mikhaylova et al., 2022; Nguyen et al., 2019), most studies have been limited to only one or two hydrotreated samples per feedstock (Celis-Cornejo et al., 2018; Guillemant et al., 2019; Le Maître et al., 2019, 2020; Li et al., 2024; Liu et al., 2016; Zhang et al., 2013), resulting in an incomplete and sometimes misleading understanding of nitrogen evolution. In particular, the HDN depth was significantly limited in the context of the RHT process (Li et al., 2021; Liu et al., 2016, 2017, 2018; Zhang et al., 2020), further hampering the understanding of the HDN process at the molecular level.

Herein, to gain a more fundamental and comprehensive understanding of the physicochemical characteristics of refractory basic and neutral nitrogen compounds during the RHT process, a series of pilot tests were carried out under diverse reaction conditions. Following this, five samples with HDN ratios ranging from 15.9% to 70.1% and their feed were selected for further analysis by ESI(+)/ESI(-) FT-ICR MS. Based on the semi-quantitative information and detailed microstructural insights derived from these samples, the refractory nature, evolution mechanisms and molecular structures of basic and neutral nitrogen compounds were well discussed.

2. Experimental sections

2.1. Feedstock and catalysts

The feedstock utilized in this study was a mixed residual oil sourced from the Anqing Branch of China Petroleum & Chemical Corporation (Sinopec). Notably, despite being a blend, the majority of its composition originated from the Shengli Oilfield. The detailed properties of this feedstock are presented in Table 1. It could be seen that the feedstock exhibits a notably high nitrogen content, reaching 0.45 wt%.

In the present study, two commercial NiMo/Al₂O₃ catalysts provided by the Catalyst Branch of Sinopec Corp were employed. The composition and properties of these catalysts, designated as HDM-CAT and HDN-CAT, are outlined in Table 2. Specifically, HDM-CAT was primarily utilized for metal removal, while HDN-CAT was focused on sulfur and nitrogen removal.

Table 1
Properties of the feedstock.

ρ^{20} , g/cm ³	0.9636	Basic nitrogen, $\mu\text{g/g}$	1475
v^{100} , mm ² /s	109.1	Ni, $\mu\text{g/g}$	27.6
CCR, wt%	9.54	V, $\mu\text{g/g}$	25.2
C, wt%	85.88	Saturates, wt%	36.7
H, wt%	11.58	Aromatics, wt%	33.5
S, wt%	1.42	Resins, wt%	28.4
N, wt%	0.450	Asphaltenes, wt%	1.4

Table 2
Composition and properties of the catalysts used in the RHT process.

Catalysts	HDM-CAT	HDN-CAT
Active species	NiMo	NiMo
Bulk density, g/cm ³	0.45	0.63
Surface area, m ² /g	165	193
Average pore diameter, nm	15	9
Pore volume, cm ³ /g	0.75	0.42

2.2. RHT tests

The RHT tests were carried out in a fixed-bed pilot plant consisting of two reactors as shown in Fig. S1. After being crushed to 16–20 mesh, the HDM-CAT and HDN-CAT catalysts were loaded sequentially into these two reactors with volumes of 225 and 275 mL, respectively.

Prior to the RHT test, the catalysts were presulfurized with gas oil containing 2.5 wt% dimethyl disulfide (DMDS) at 230, 280 and 320 °C for 4 h each at a liquid hourly space velocity (LHSV) of 0.30 h⁻¹, a hydrogen pressure of 16 MPa, and a hydrogen-to-oil ratio of 700 (v/v). After sulfidation, the catalysts were stabilized for 240 h at a temperature of 386 °C, a LHSV of 0.17 h⁻¹, a hydrogen pressure of 16 MPa, and a hydrogen-to-oil ratio of 700 (v/v). The RHT tests were then conducted under the following conditions: a temperature of 366–406 °C, a LHSV of 0.10–0.25 h⁻¹, a hydrogen pressure of 14–17 MPa, and a hydrogen-to-oil ratio of 300–1200 (v/v). For each test, samples were collected from both reactor effluents and designated as HDM product and HDN product, respectively.

2.3. ESI(+)/ESI(-) FT-ICR MS analysis

The residual oil and its hydrotreatment products were all dissolved in toluene and prepared as solutions at a concentration of 10 mg/mL each. These solutions were then diluted in duplicate to 0.5 mg/mL with a toluene/methanol (1:1, v/v) solvent mixture. All solvents used were of chromatographic grade. Prior to mass spectrometric analysis, formic acid (at 1% of the volume of the sample solution) was added to the diluted samples to facilitate ESI(+), while aqueous ammonia (at 2% of the volume of the sample solution) was added to the parallel samples to facilitate ESI(-).

The prepared samples were all analyzed on a 15 T Bruker Solarix XR FT-ICR MS equipped with an electrospray ionization source. Nitrogen gas (99.999%) was used as both the nebulizing and drying gas, with flow rates set at 1.0 and 2.0 L/min, respectively. The source temperature was maintained at 200 °C. In ESI(+) mode, samples were injected into the ionization source at a flow rate of 240 $\mu\text{L/h}$ using a syringe pump. The voltages for the capillary, end plate offset and capillary outlet were set to -4500, -500, and 220 V respectively. The RF amplitudes for the funnel and octopole were 150 and 400 Vpp, respectively. The ion accumulation time was set to 0.1 s. The time of flight (TOF) in the transfer optics was configured to 0.8 ms. The mass range was set to cover m/z 100–1500 Da. The data

size was 8 M, with each spectrum measured by 64 scans. In ESI(-) mode the sample injection rate was 360 $\mu\text{L/h}$. The voltage for the capillary was set to 4000 V. The RF amplitude for the octopole was 450 Vpp. The ion accumulation time was 3.0 s. Each spectrum was measured with 128 scans.

2.4. Data analysis

In the processing of nitrogen contents data, neutral nitrogen contents are calculated by subtracting basic nitrogen contents from total nitrogen contents. During the processing of mass spectra data, peaks were selected based on relative abundance exceeding five standard deviations of the baseline root-mean-square noise. Molecular formulas were assigned in the broadband spectra by matching the accurate m/z values, with a relative error tolerance of less than 1 ppm. These formulas were expressed as $\text{C}_c\text{H}_h\text{N}_n\text{O}_o\text{S}_s$, where the subscripts represent the number of atoms for each element. Additionally, the DBE was calculated using the formula $\text{DBE} = c - h/2 + n/2 + 1$. Suppose the ion signal intensity corresponding to a certain mass-to-charge ratio m_k/z_i is $I_{k,i}$, the relative abundance of this ion can be calculated as $RA_{k,i} = I_{k,i}/\sum I_{k,i}$. The relative abundance of nitrogen compounds with a DBE of j can be calculated as $RA_{k,j} = \sum I_{k,j}/\sum I_{k,i}$, and the relative abundance of nitrogen compounds with a carbon number of c can be calculated as $RA_{c,i} = \sum I_{c,i}/\sum I_{k,i}$. The pseudo basic and neutral nitrogen contents were obtained by multiplying their relative abundances by the corresponding nitrogen contents in the samples. The pseudo removal ratios were calculated based on the pseudo contents.

3. Results and discussion

3.1. Removal of basic and neutral nitrogen during the RHT process

To illustrate the resistant characteristics of nitrogen compounds throughout the RHT process, Fig. 1 shows the impact of reaction temperature, LHSV, hydrogen-to-oil ratio, and hydrogen pressure on the final removal ratios of total, basic, and neutral nitrogen, designated as HDN, HDBN, and HDNN respectively. Notably, the HDN ratios were primarily influenced by reaction temperature and LHSV, followed by hydrogen pressure, with the hydrogen-to-oil ratio having the least influence. However, despite the severe reaction conditions employed in the tests, the HDN ratios remained limited, peaking at 75.7%. Furthermore, the selectivity of the reaction for removing basic and neutral nitrogen was influenced distinctively by varying the reaction parameters. Specifically, the HDBN ratio increased more rapidly than the HDNN ratio with increasing temperature, whereas the HDNN ratio exceeded the growth rate of the HDBN ratio with increasing hydrogen pressure. This observation aligns with the reported trends in the hydro-treating process of nitrogen model compounds (Nagai and Masunaga, 1988).

However, as Fig. 2 demonstrates, the selectivity of the reaction for removing basic and neutral nitrogen compounds may behave more as a function of the HDN levels. With increased HDN ratios, both HDNN and HDBN ratios increased. Furthermore, the HDNN ratio exceeded the HDN ratio initially, while the HDBN ratio remained low or even turned negative, indicating an increase in the basic nitrogen. When the HDN ratios exceeded about 40%, the trend reversed. Consequently, the proportion of basic nitrogen initially rose and then declined as the HDN ratio increased. This trend has also been observed in the hydrotreating processes of several VGOs and CGOs (Mikhaylova et al., 2022; Nguyen et al., 2019). This phenomenon can be attributed, at least in part, to converting

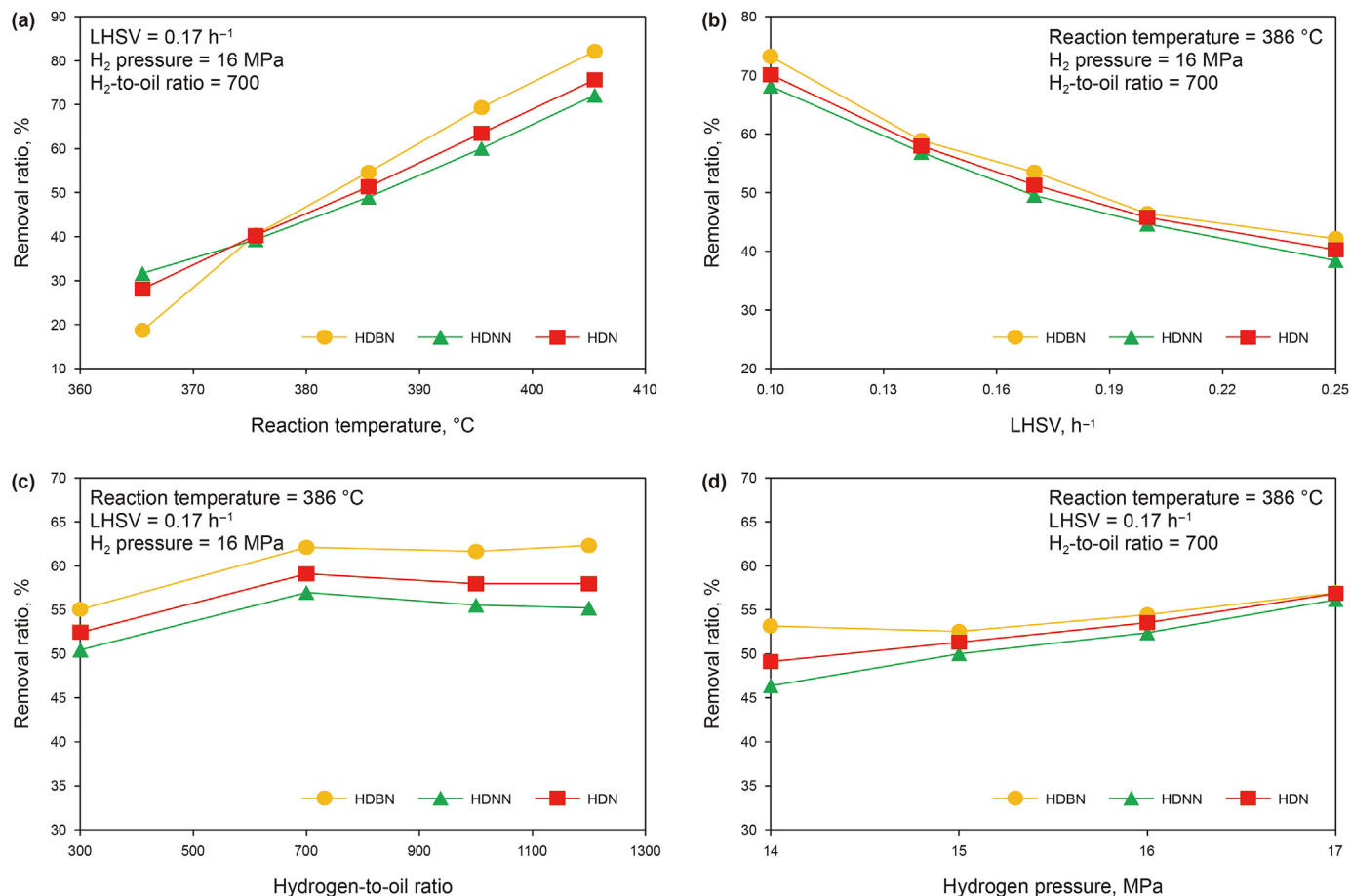


Fig. 1. Effects of (a) reaction temperature, (b) LHSV, (c) hydrogen-to-oil ratio, and (d) hydrogen pressure on the nitrogen removal ratio of HDN products.

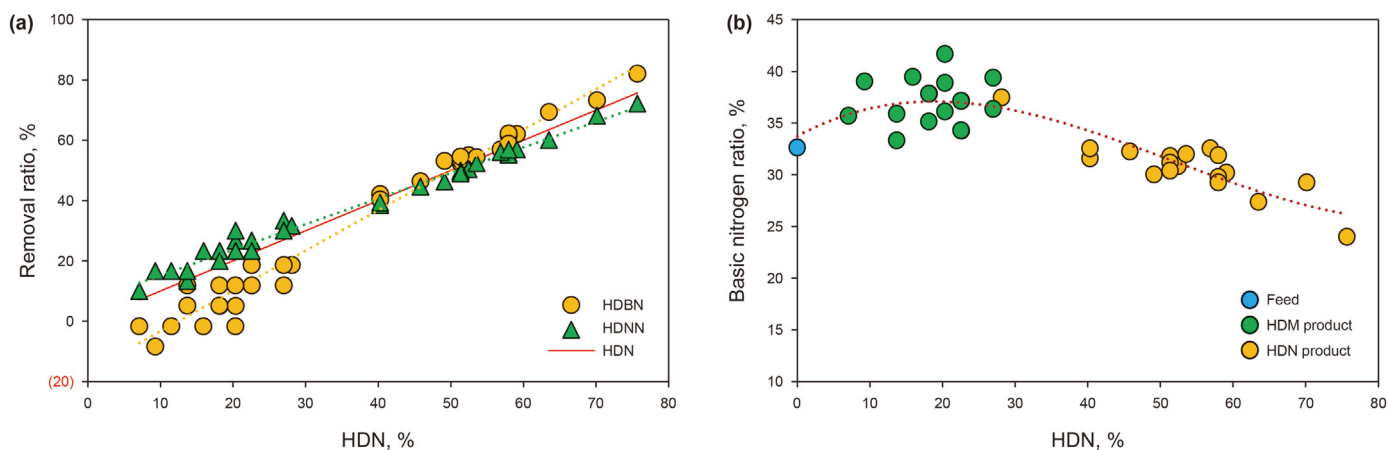


Fig. 2. Change of (a) basic and neutral nitrogen removal ratios, (b) proportion of basic nitrogen as a function of HDN level.

neutral nitrogen compounds into basic ones during hydro-processing (Bello et al., 2021; Mikhaylova et al., 2022; Prado et al., 2017). Notably, in a RHT process with HDN ratios ranging from 3.7% to 55.6%, the basic nitrogen ratio consistently decreased as the HDN level increased (Li et al., 2021). This could be due to the high initial basic nitrogen ratio of 37.8% in the feedstock. Regardless, these observations highlight the intricate and fascinating HDN mechanisms during the RHT process, which will be further explored at the molecular level in the subsequent sections.

3.2. Evolution characteristics of basic and neutral nitrogen compounds

To gain insight into the intricate HDN reaction mechanism during the RHT process, the feed and its five hydrotreated samples with HDN ratios ranging from 15.9% to 70.1% were chosen for molecular-level analysis by ESI(+)/ESI(-) FT-ICR MS. The reaction conditions and key properties of these hydrogenated samples are presented in Table 3. The mass spectra and free induction decay of

Table 3
Reaction conditions and key properties of the hydrogenated samples.

Sample	Sample1	Sample2	Sample3	Sample4	Sample5
Sample type	HDM	HDN	HDN	HDN	HDN
Reaction conditions					
Reaction temperature, °C	386	386	386	386	386
LHSV, h ⁻¹	0.38	0.25	0.20	0.14	0.10
Hydrogen pressure, MPa	16	16	16	16	16
Hydrogen-to-oil ratio, v/v	700	700	700	700	700
Key properties					
N, wt%	0.380	0.270	0.245	0.190	0.135
Basic nitrogen, µg/g	1500	853	790	606	395
HDN, %	15.9	40.3	45.8	58.0	70.1

both the feed and its three hydrogenated samples are shown in Figs. S2–S5. The nitrogen-containing species identified as basic and neutral ones by ESI(+) and ESI(−) FT-ICR MS are shown in Fig. 3. Within the feedstock, the nitrogen compounds identified encompassed the classes N1, N2, N1S1, N1O1, N1O2, and N1S1O1. Notably, the N1 class dominated both the basic and neutral nitrogen species, with relative abundances of 72.0% and 69.0%, respectively. After undergoing hydrotreatment, the N1S1 and N1S1O1 classes were reduced to near zero in all samples. Furthermore, the N2 class was eliminated when the HDN ratio reached 40.3%. Previous reports suggested that these compounds may be converted to the N1 class compounds during the hydrotreating process (Li et al., 2021, 2024; Zhang et al., 2013). The primary nitrogen-containing compounds remaining in the hydrotreated samples were the N1, N1O1, and N1O2 classes, which have also been observed in previous studies (Guillemet et al., 2020; Li et al., 2021, 2024; Liu et al., 2016; Zhang et al., 2013). As the N1 class was the most abundant in all hydrotreated samples, with relative abundances ranging from 92.1% to 96.4%, the present investigation primarily focused on this class.

Fig. 4 illustrates the relationship between DBE and carbon number for the identified basic and neutral N1 class compounds presented in the feedstock and its two hydrotreated samples, exhibiting HDN ratios of 15.9% and 70.1%, respectively. In addition, we have provided separate plots for the aforementioned feed and products in Fig. S6 to enhance clarity and facilitate a more detailed analysis. In the feedstock, the DBE of the basic nitrogen compounds ranged from 4 to 24, with the most abundant ones ranging from 8 to 11, peaking at 10. The carbon number of these compounds varied from 15 to 65, with the primary abundance between 24 and 35 and

peaking at 28. Meanwhile, the neutral nitrogen compounds exhibited a DBE ranging from 6 to 26, displaying bimodal peaks at 9 and 12. The carbon number of these compounds spanned from 14 to 80, with the main abundance between 30 and 39 and a peak at 35. Following hydrotreatment, a significant reduction in both basic and neutral nitrogen compounds with high DBEs was observed, with some nitrogen compounds being eliminated. This observation aligns with findings from other hydrotreating processes of heavy oils (Liu et al., 2016, 2017; Mikhaylova et al., 2022). Meanwhile, many basic N1 class compounds with DBEs ranging from 2 to 3 emerged in the hydrotreated samples. This could be attributed to the partial hydrogenation of basic nitrogen compounds or the conversion from neutral ones (Bello et al., 2021; Li et al., 2021; Liu et al., 2016, 2018; Mikhaylova et al., 2022; Nguyen et al., 2019; Zhang et al., 2013). Interestingly, neutral N1 class compounds with DBE less than 6 were absent from the hydrotreated samples, suggesting that the neutral nitrogen compounds with DBE less than 6 may all be converted into basic ones during the hydrotreatment process.

When the influence of carbon number is taken into account, the situation becomes more complicated. As shown in Fig. 4, many neutral nitrogen compounds with high carbon numbers were eliminated, while a significant number of basic nitrogen compounds with carbon numbers up to 70 appeared in the hydrotreated samples. This suggests that these basic nitrogen compounds may have originated, at least in part, from the disappearing neutral nitrogen compounds and multi-heteroatom compounds (Bello et al., 2021; Li et al., 2021; Liu et al., 2016, 2018; Mikhaylova et al., 2022; Nguyen et al., 2019; Zhang et al., 2013). In addition, both the basic and neutral nitrogen compounds with low carbon numbers were dramatically removed, with some being eliminated, which is consistent with some earlier research (Al-Hajji et al., 2008; Liu et al., 2016, 2018; Mikhaylova et al., 2022; Zhang et al., 2013). In more detail, as shown by Cho et al. (2011), the planar limit of the DBE/carbon number plot by linear addition of aromatic rings is 0.75, thus the relationship between DBE and carbon number for pyridine and its derivatives could be expressed as $y = 0.75x + 0.25$ (Fig. 4(a)), while the corresponding relationship for pyrrole and its derivatives could be expressed as $y = 0.75x$ (Fig. 4(b)). Using this approach, it could be seen that at HDN ratios of 15.9% and 70.1%, the easy-to-convert basic nitrogen compounds were those with alkyl chains of C1–C5

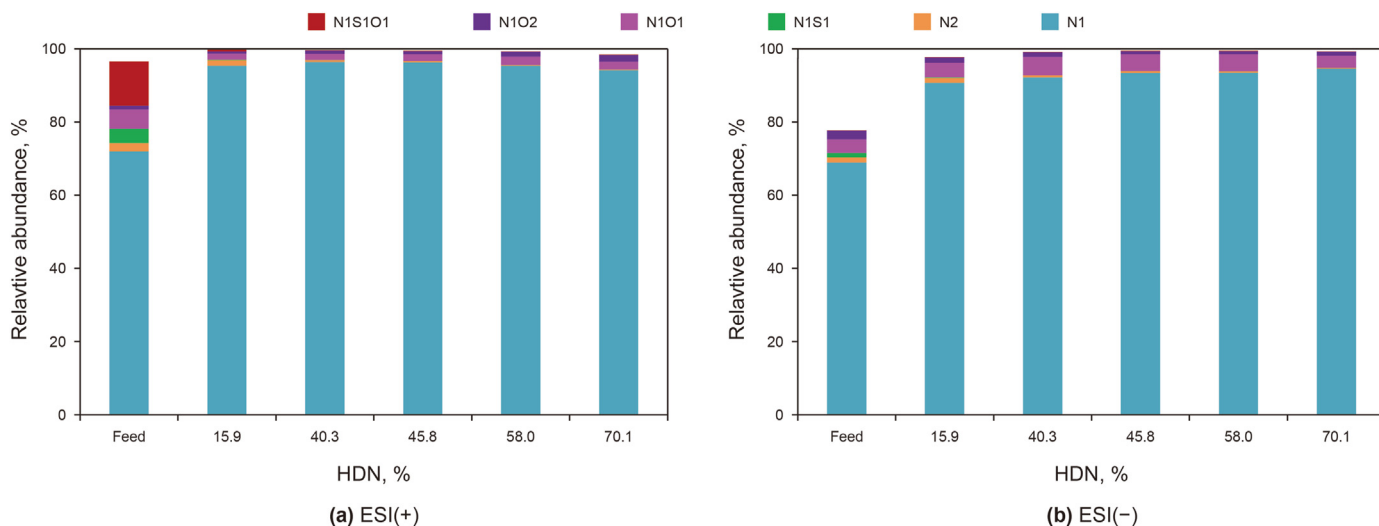


Fig. 3. Chemical classes of (a) basic nitrogen, and (b) neutral nitrogen as a function of HDN level.

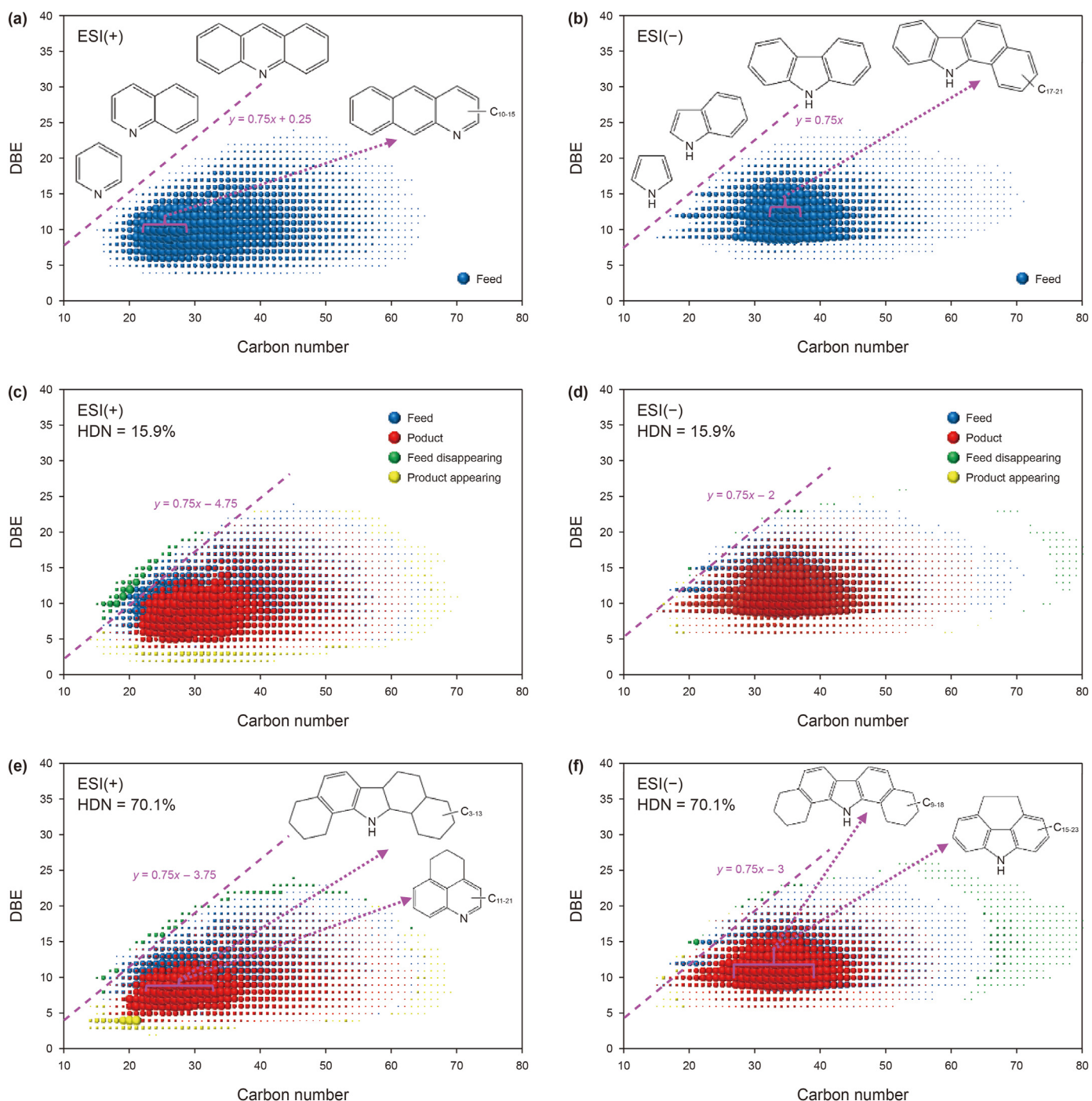


Fig. 4. Plots of DBE versus carbon number for basic and neutral N1 compounds in the feed and its two hydrotreated samples. The bubbles of feed disappearing and product appearing were increased five times to get a clear sight. The skeletons are shown only for illustrative purposes.

and C1–C4, while the corresponding neutral nitrogen compounds were those with alkyl chains of C1–C2 and C1–C3, respectively. Moreover, at the highest HDN ratio of 70.1%, the most abundant basic nitrogen compounds had a DBE of 8 and a carbon number ranging from 23 to 33. On the other hand, the most common neutral nitrogen compounds had DBEs of 10 and 11, and a carbon number ranging from 28 to 39. These observations indicate that during the RHT process, at least some basic nitrogen compounds in the hydrogenated samples were converted from neutral ones. Furthermore, the reactivity of the basic nitrogen compounds is

more sensitive to the alkyl carbon number than the neutral ones. These phenomena lead to significant differences in both DBE and carbon number for the refractory basic and neutral nitrogen compounds, which should be better understood by a thorough investigation of the DBE and carbon number aspects.

3.3. Reactivity of basic and neutral nitrogen compounds based on DBE

Before analyzing the removal process of basic and neutral

nitrogen compounds based on DBE, it is crucial to note that the nitrogen compounds with the same DBE value are a group of numerous compounds with different reactivities, and the reactivity of the DBE-based nitrogen families has usually been referred to as their average value. Fig. 5 shows the relationship between the pseudo contents of the basic and neutral nitrogen and DBE for the feed and its three hydrogenated samples, each exhibiting distinct HDN ratios. As shown in Fig. 5(a), after hydrotreatment, the DBE distributions of the basic nitrogen compounds shifted to lower values, with a peak shifting from 10 to 8. The reduction of 2 for DBE likely corresponds to the hydrogenation of a condensed aromatic ring (Mikhaylova et al., 2022; Nguyen et al., 2019). Meanwhile, some basic nitrogen compounds with high DBEs and DBEs ranging from 2 to 3 appeared in the hydrotreated samples. Furthermore, at the lowest HDN ratio of 15.9%, the pseudo contents of basic nitrogen compounds with DBEs ranging from 2 to 9 were higher than those in the feed. These phenomena highlight the partial hydrogenation of basic nitrogen compounds or their conversion from

neutral nitrogen compounds (Mikhaylova et al., 2022; Nguyen et al., 2019). With a further increase in HDN, the DBE distribution of basic nitrogen compounds became narrower. At the highest HDN ratio of 70.1%, the remaining major basic nitrogen compounds had DBEs ranging from 7 to 9, with the peak remaining at 8.

As shown in Fig. 5(b), before hydrotreatment, the neutral nitrogen compounds exhibited a bimodal DBE distribution with peaks at 9 and 12. After hydrotreatment, this distribution transformed into an unimodal pattern centered at 10. Notably, certain neutral nitrogen compounds with high DBEs disappeared, indicating that compounds with high aromaticity possess greater reactivity (Guillemant et al., 2019; Lai et al., 2020; Le Maître et al., 2019, 2020; Liu et al., 2018; Mikhaylova et al., 2022; Zhang et al., 2013). Additionally, at HDN ratios of 15.9% and 40.3%, the pseudo contents of neutral nitrogen compounds with DBE ranging from 6 to 8 and 10 to 11 surpassed those in the feedstock, suggesting partial hydrogenation of neutral nitrogen compounds with high DBEs (Mikhaylova et al., 2022; Nguyen et al., 2019). As the HDN

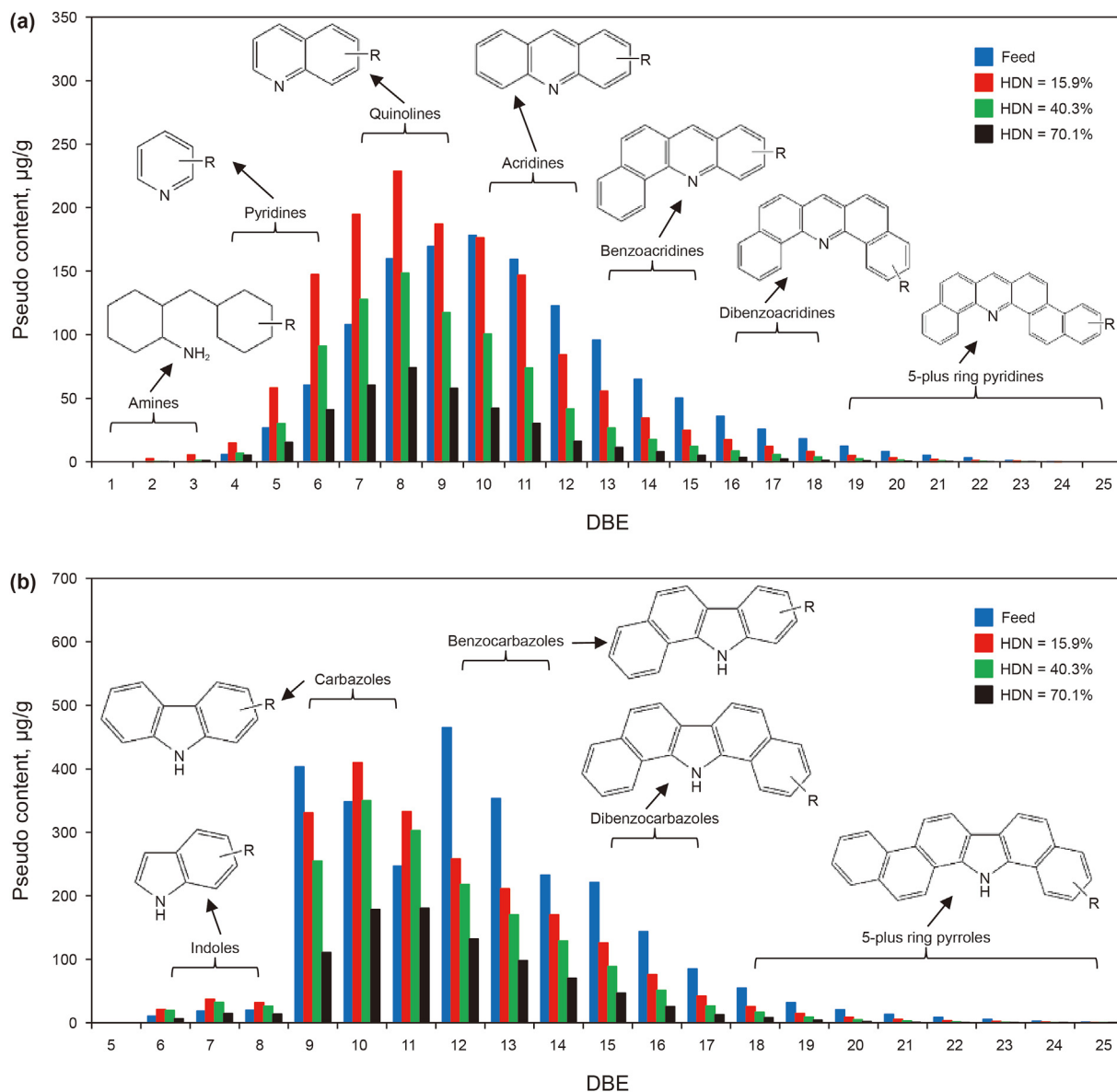


Fig. 5. Plots of pseudo contents of (a) basic nitrogen, and (b) neutral nitrogen versus DBE for the feed and its three hydrotreated samples. The skeletons are shown only for illustrative purposes.

ratios increased, a greater number of neutral nitrogen compounds with high DBE values disappeared. At the highest HDN ratio of 70.1%, the predominant neutral nitrogen compounds possessed DBEs between 10 and 11, with the peak shifting to 11. Notably, the pseudo contents of neutral nitrogen compounds with DBEs of 6–8 were significantly lower than those with DBEs of 9 and 10 in all hydrogenated samples. This observation implies that the neutral nitrogen compounds may be converted into basic nitrogen compounds rather than neutral ones with DBEs of 6–8.

For a more quantitative understanding of the reactivity of nitrogen compounds, the basic and neutral nitrogen compounds in the residual oils were grouped into 7 and 5 families, respectively, according to their DBE values, as shown in Fig. 5. Using this lumping method, the relationship between the pseudo contents of nitrogen families and the HDN ratios are shown in Fig. 6. As shown in Fig. 6(a), in the feed, the amines were not identified, while the pseudo contents of other basic nitrogen families decreased in the order of acridines > quinolines > benzoacridines > dibenzoacridines > pyridines > 5-plus ring pyridines. After undergoing hydrotreatment, the pseudo contents of 5-plus ring pyridines, dibenzoacridines, benzoacridines, and acridines decreased continuously with increasing HDN levels, whereas the pseudo contents of quinolines, pyridines, and amines first increased and then decreased. At the highest HDN ratio of 70.1%, the pseudo contents of the left basic nitrogen families decreased in the following order: quinolines > acridines > pyridines > benzoacridines > dibenzoacridines > 5-plus ring pyridines > amines. These observations were consistent with those reported in previous studies (Mikhaylova et al., 2022; Nguyen et al., 2019). Regarding the neutral nitrogen families, as illustrated in Fig. 6(b), the pseudo contents of these families initially decreased in the order of benzocarbazoles > carbazoles > dibenzocarbazoles > 5-plus ring pyrroles > indoles. With increasing HDN ratios, the pseudo contents of 5-plus ring pyrroles, dibenzocarbazoles, and benzocarbazoles decreased continuously, whereas the pseudo contents of carbazoles and indoles initially increased before decreasing. Especially, in the most severely-hydrogenated sample, the sequence of decrease in pseudo contents among the remaining neutral nitrogen families was as follows: carbazoles, benzocarbazoles, dibenzocarbazoles, indoles, and 5-plus ring pyrroles. These observations were similar to those in previous work (Mikhaylova et al., 2022; Nguyen et al., 2019).

Unfortunately, the calculation of nitrogen family removal ratios based on their pseudo contents is not feasible due to the inability to accurately estimate the net formation contents of these compounds

during the RHT process. Nevertheless, Fig. 7 presents a comparative analysis of the pseudo contents of nitrogen families in the hydrogenated sample with the highest ratio of 70.1%. The pseudo contents of the remaining nitrogen families exhibit a descending trend as follows: carbazoles, benzocarbazoles, quinolines, acridines, dibenzocarbazoles, pyridines, indoles, 5-plus ring pyrroles, benzoacridines, dibenzoacridines, 5-plus ring pyridines, and amines. It should be noted that the decreasing order of reactivity of nitrogen compounds was not the same as that proposed in a previous review (Bello et al., 2021), which may be due to the intricate HDN mechanisms of real oil. The refractory nature of basic and neutral nitrogen compounds can be attributed to several factors. Firstly, basic nitrogen compounds exhibit superior adsorption properties compared to neutral ones (Bello et al., 2021; Furimsky and Massoth, 2005). Secondly, nitrogen compounds with increased molecular weight, aromaticity, and alkyl substitutions near the nitrogen atom tend to exhibit lower reactivity, resulting from decreased intrinsic reactivity and/or increased diffusion resistance (Bello et al., 2021; Furimsky and Massoth, 2005; Le Maître et al., 2020). Thirdly, nitrogen compounds with high aromaticity often demonstrate preferential adsorption on catalysts (Furimsky and Massoth, 2005) and a reduced likelihood of alkyl substitutions near the nitrogen atom. Considering these factors, amines and pyridines within the basic nitrogen families, as well as indoles within the neutral nitrogen families, which possess the highest intrinsic reactivities and/or the lowest steric hindrance, are expected to undergo significant removal. Conversely, the reactivity order of the remaining basic and neutral nitrogen families may decline due to diminishing adsorption advantages. Surprisingly, we observed that the pseudo contents of quinolines and pyridines were higher than those of acridines and indoles, respectively. A plausible explanation for this phenomenon is that the partially hydrogenated nitrogen compounds resulting from the net formation might have considerable concentrations, potentially having a significant influence on the observed reactivity patterns of the nitrogen families. To unravel this mystery, a thorough examination of the intricate reaction pathway of nitrogen compounds is required.

3.4. Reaction mechanisms of basic and neutral nitrogen compounds

During the HDN process, if cracking reactions are ignored, the primary change that occurs in DBE shifts can be attributed to hydrogenation and ring-opening reactions, without any alteration in carbon number (Mikhaylova et al., 2022; Nguyen et al., 2019). Fig. S7 illustrates the reaction networks for carbazole and acridine,

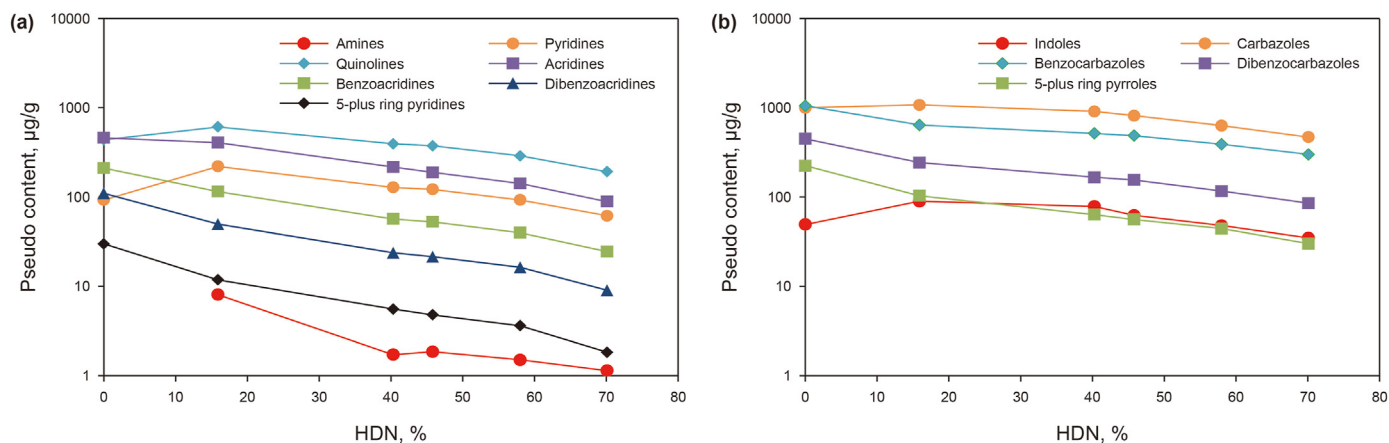


Fig. 6. Plots of pseudo contents of (a) basic nitrogen families, and (b) neutral nitrogen families as a function of HDN level.

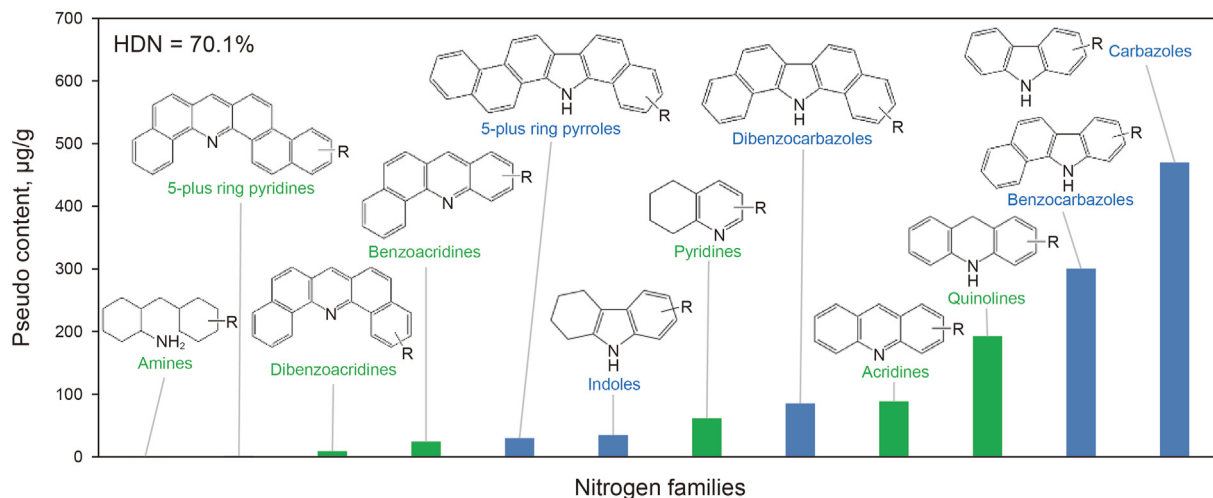


Fig. 7. Plots of pseudo contents of nitrogen families in the hydrotreated sample with the highest HDN ratio. The skeletons are shown only for illustrative purposes.

described by DBE and carbon number (Bello et al., 2021; Furimsky and Massoth, 2005). It could be seen that during the HDN process, hydrogenation of an isolated aromatic ring and a condensed aromatic ring can lead to DBE shift values of -3 and -2 , respectively. Additionally, ring-opening reaction and hydrogenation of a five-member ring in neutral nitrogen compounds can lead to a DBE shift value of -1 (Mikhaylova et al., 2022; Nguyen et al., 2019). As depicted in Fig. 5, both basic and neutral nitrogen compounds exhibited a distinct DBE shift during the RHT process, signifying the transformation of nitrogen compounds with higher DBEs into species with lower DBEs. Notably, at the lowest HDN ratio of 15.9%, basic nitrogen compounds with DBEs of 2–9 display higher pseudo contents compared to those in the feed, suggesting their role as intermediates during the HDN process. For example, amines presented in the products with DBEs of 2–3 could be the ring-opening products of fully saturated compounds originating from those with 3 and 4 rings, respectively (Fig. S7). Furthermore, octahydroacridines with a DBE of 6 could be the products of partially hydrogenated tetrahydroacridine (DBE = 8) and acridine (DBE = 10) (Mikhaylova et al., 2022; Nguyen et al., 2019). Interestingly, these intermediates are prominently observed in all hydrogenated samples, indicating that the HDN mechanisms of residual oil may be similar to those revealed by model compounds (Bello et al., 2021; Furimsky and Massoth, 2005; Nguyen et al., 2019). Regrettably, we encountered significant challenges in tracking the complete reaction pathway of basic nitrogen compounds based on the available information, partly due to the transformation of neutral nitrogen compounds into basic ones (Bello et al., 2021; Li et al., 2021; Liu et al., 2016, 2018; Mikhaylova et al., 2022; Nguyen et al., 2019; Zhang et al., 2013). Nevertheless, there appears to be sufficient evidence to infer the reaction mechanisms of neutral nitrogen compounds.

Fig. 8 illustrates the pseudo contents versus DBE for the basic and neutral nitrogen compounds with constant carbon numbers as a function of HDN levels. At the lowest HDN ratio of 15.9%, the basic nitrogen compounds with carbon numbers 19 to 21 were reduced to extremely low pseudo content levels, nearly approaching complete elimination. As the HDN ratio increased, the pseudo contents of these compounds initially increased before decreasing, mostly exceeding those at the HDN ratio of 15.9%. The basic nitrogen compounds appearing with HDN ratios higher than 15.9% could have originated from multi-heteroatom compounds, neutral nitrogen compounds, or basic nitrogen compounds with higher carbon numbers (Bello et al., 2021; Li et al., 2021; Liu et al., 2016, 2018;

Mikhaylova et al., 2022; Nguyen et al., 2019; Zhang et al., 2013). However, it was observed that most multi-heteroatom compounds underwent conversion during the initial HDN process. Furthermore, cracking reactions were not central to our findings, since the samples analyzed by FT-ICR MS were collected at a moderate 386 °C across various LHSV. Additionally, the divergent variation patterns between neutral nitrogen compounds and basic ones with the same carbon number strongly suggest that cracking was not the primary driver of the overall reaction dynamics. Therefore, we hypothesized that these basic nitrogen compounds, which appeared with HDN ratios higher than 15.9%, were primarily derived from neutral nitrogen compounds with the same carbon numbers. Detailed analysis revealed that the pseudo contents of neutral nitrogen compounds with carbon numbers ranging from 19 to 23 in the feed typically exhibited two or three peaks at DBE of 9, 12, and 15. Following hydrotreatment, the most common neutral nitrogen compounds were those with a DBE of 10, which could be derived from those with a DBE of 12. Additionally, the neutral nitrogen compounds with a DBE of 15 were transformed into those with a DBE of 13 and subsequently 11. Notably, the neutral nitrogen compounds with DBEs between 6 and 8 were significantly less abundant than those with higher DBEs, suggesting that neutral nitrogen compounds with a DBE of 9 or higher were primarily converted into basic ones through the hydrogenation of an isolated aromatic ring. Consequently, after hydrotreatment, the basic nitrogen compounds were predominantly present at DBEs of 7–8, partly originating from neutral nitrogen compounds with DBEs ranging from 10 to 11. Additionally, it was observed that the basic nitrogen compounds with DBEs of 7–8 underwent further hydrogenation before denitrogenation. For carbon number 21, a peak at a DBE of 6 was observed for the basic nitrogen compounds. This suggests that the ring-opening reaction of the five-membered nitrogen ring could occur before the hydrogenation of the final aromatic ring. During the investigation of nitrogen model compounds, it was discovered that the primary reaction pathway for carbazole involves opening the five-membered nitrogen ring before hydrogenating the final aromatic ring (Bello et al., 2021; Nagai and Masunaga, 1988). This study confirmed the presence of intermediates from both typical reaction pathways for neutral nitrogen compounds in the RHT process. Moreover, as shown in Fig. 5, at the highest HDN ratio of 70.1%, the pseudo contents of basic nitrogen compounds with DBEs below 5 were significantly lower than those with DBEs of 6–8. This suggests that the primary reaction pathway for neutral nitrogen compounds in residual oil may

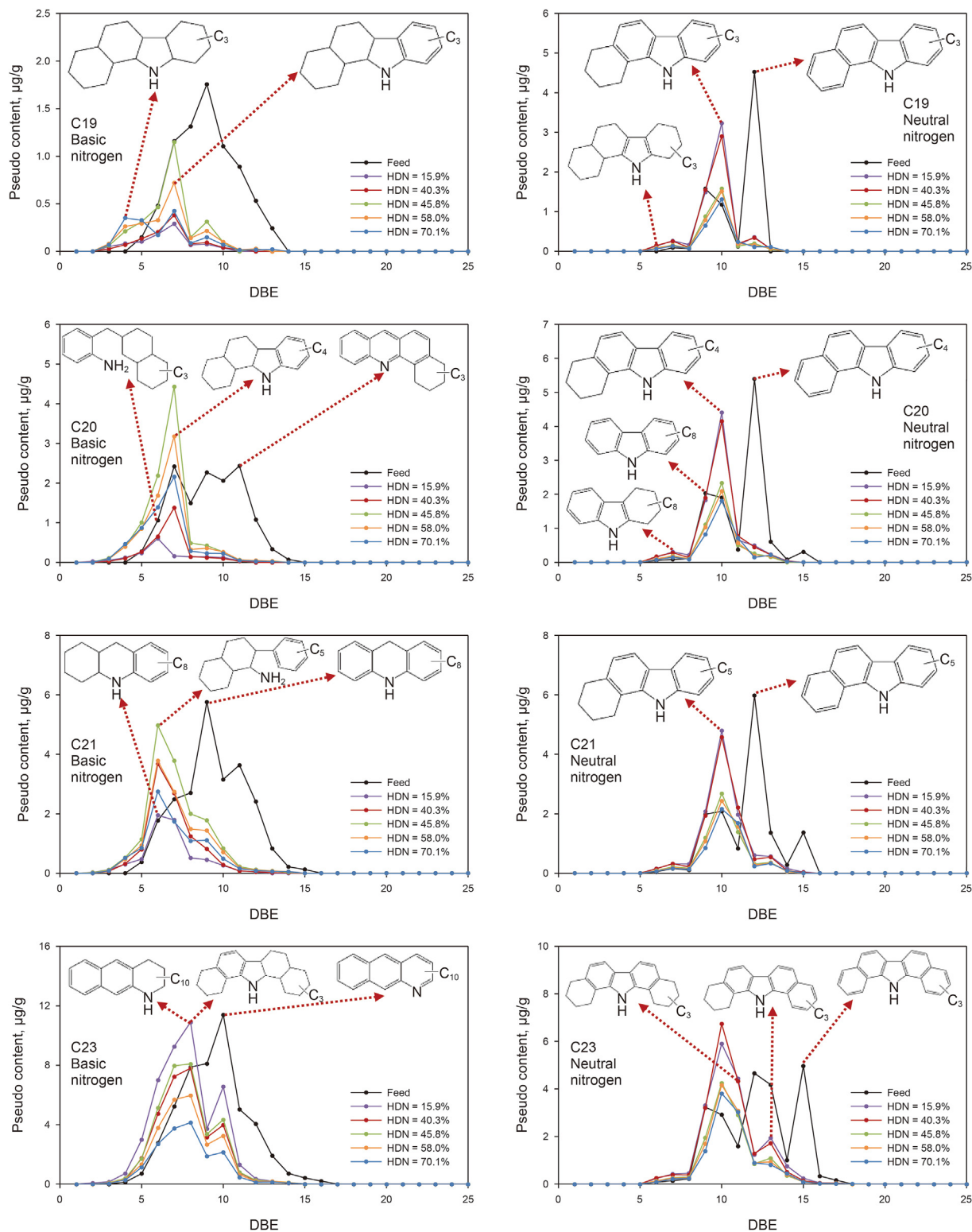


Fig. 8. Plots of DBE distributions for the basic and neutral nitrogen compounds with constant carbon numbers as a function of HDN ratio. The skeletons are shown only for illustrative purposes.

be consistent with the model compounds.

Based on these findings, we have proposed the reaction mechanisms for benzocarbazoles and dibenzocarbazoles in Fig. 9. In general, nitrogen compounds with multiple aromatic rings saturate the rings sequentially from the outside inwards to the last ring. Then, the compounds either undergo ring-opening and denitrogenation

directly or saturate the last aromatic ring first, with the former being the dominant pathway. It should be noted that the removal process of these neutral nitrogen compounds involves carbazoles and quinolines as the principal intermediates. This may explain why quinolines were more abundant than acridines even at the highest HDN level. Despite previous studies suggesting that the refractory nature

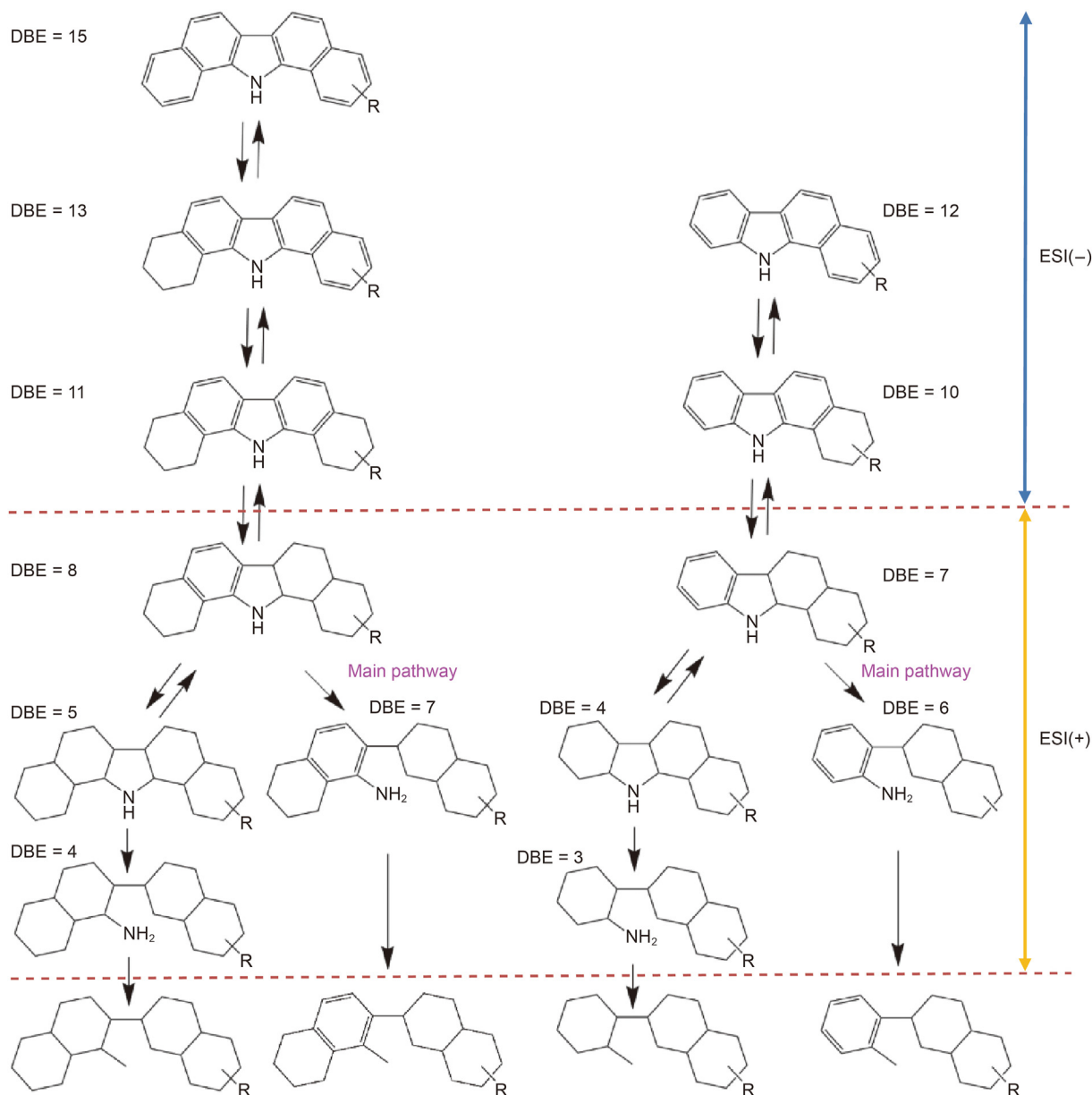


Fig. 9. Reaction networks of dibenzocarbazoles and benzocarbazoles with the description of DBE.

of carbazoles could be attributed to their role as intermediates during the removal process of neutral nitrogen compounds with high DBEs (Mikhaylova et al., 2022), we believed this might not be the predominant reason. Fig. S8 shows the pseudo removal ratios of the neutral nitrogen families by considering the pseudo contents of the feed as the sum of the original contents in the feed and the net formation contents of neutral nitrogen compounds with higher DBEs. This calculation may slightly overestimate the pseudo removal ratios of the neutral nitrogen families with low DBEs, because the neutral nitrogen compounds rich in naphthenic rings can undergo ring opening and denitrogenation reactions without further hydrogenation. However, it could be seen that the pseudo removal ratios of the carbazoles, although somewhat overestimated, were still the lowest at all HDN levels. Based on these findings, we postulated that the primary refractory nature of carbazoles may be due to their low aromaticity and high steric hindrance.

3.5. Influence of carbon number on the reactivities of the basic and neutral nitrogen compounds

Apart from the preeminent influence of aromaticity, the carbon number also has a notable influence on the reactivity of nitrogen compounds. Before analyzing the variation in carbon number distribution, it is important to note that significant changes in the distribution can occur due to severe alkyl chain cracking or sharp differences in the conversion rates of different alkylated nitrogen compounds (Nguyen et al., 2019). Fig. 10 displays the pseudo contents of basic and neutral nitrogen compounds versus carbon number with different HDN levels. The feedstock contained basic nitrogen compounds with carbon numbers ranging from 15 to 65, with the majority between 24 and 35 and peaking at 28. Upon hydrotreatment, the basic nitrogen compounds with carbon numbers less than 20 were almost completely consumed, while those with carbon numbers higher than 65 were detected in the

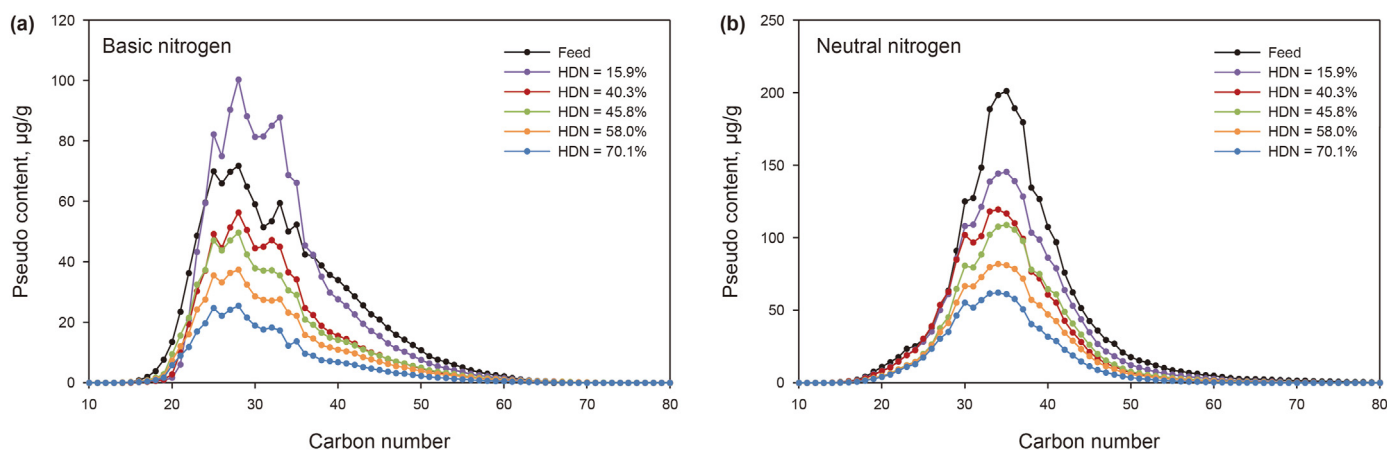


Fig. 10. Plots of pseudo contents of (a) basic nitrogen compounds and (b) neutral nitrogen compounds versus carbon number for the feed and its hydrogenated samples.

hydrogenated samples. At the lowest HDN ratio of 15.9%, the basic nitrogen compounds with carbon numbers ranging from 25 to 36 had higher pseudo contents than those in the feed. These compounds could have been converted from neutral nitrogen compounds and/or multi-heteroatom compounds (Li et al., 2021, 2024; Zhang et al., 2013). Furthermore, as the HDN ratios continued to increase, the high-carbon basic nitrogen compounds were removed more rapidly than the low-carbon ones. At the highest HDN level of 70.1%, the basic nitrogen compounds were primarily abundant with carbon numbers ranging from 23 to 33, with the peak remaining at 28. Regarding the neutral nitrogen compounds, they had carbon numbers ranging from 14 to 80, with the majority between 30 and 39 and a peak at 35. During hydrotreatment, neutral nitrogen compounds with higher carbon numbers showed greater reactivity, resulting in a shift towards lower carbon numbers with increasing HDN levels, except for those with the lowest carbon numbers. In the most severe hydrogenated sample, neutral nitrogen compounds were most abundant at carbon numbers 28 to 39, with a peak at 34. In more detail, Fig. S9 presents the carbon number distributions of several key DBE-based basic nitrogen compounds across varying HDN levels. Basic nitrogen compounds with a medium carbon number ranging from 20 to 38 tended to accumulate significantly when the DBE value was below 13, particularly at the lowest HDN ratio of 15.9%. As the HDN levels increased, the accumulation of these compounds diminished. Furthermore, the basic nitrogen compounds with lower carbon numbers were significantly eliminated, and this elimination intensified as the DBE value increased. Meanwhile, the high-carbon basic nitrogen compounds were removed at higher rates than the medium-carbon compounds. In summary, the reactivity of basic nitrogen compounds initially decreased with increasing carbon numbers and then increased. The carbon number distributions of neutral nitrogen compounds exhibited similar trends to those of basic nitrogen compounds, as evident in Fig. S10. However, while the removal of low-carbon neutral nitrogen compounds was less pronounced than that of basic ones, the removal of high-carbon neutral nitrogen compounds was more significant.

These observations implied that nitrogen compounds with higher carbon numbers typically exhibited greater reactivity, except for those with the lowest carbon numbers. Nevertheless, while this finding is supported by prior research (Celis-Cornejo et al., 2018; Liu et al., 2016; Mikhaylova et al., 2022), it is important to acknowledge that steric hindrance may rise with an increase in carbon number. Therefore, further investigation is required to gain a comprehensive understanding of this trend. One plausible

explanation is that nitrogen compounds with high carbon numbers undergo conversion to medium or low-carbon compounds through long-side chain cracking before further transformation (Liu et al., 2017). However, given that the cracking reactions may not be intense during the collection of these samples due to the moderate reaction temperature, we considered another factor that could significantly influence this process. It is important to know that the influence of alkyl chains on the reactivity of nitrogen compounds depends on their substitution positions rather than merely their carbon numbers. Specifically, alkyl substitutions adjacent to the nitrogen atom may lead to reduced reactivity due to heightened steric hindrance (Le Maître et al., 2020). Moreover, Liu et al. (2019) demonstrated that sulfur compounds sharing the same DBE tend to possess more naphthenic-aromatic structures as their carbon numbers increase. Therefore, we hypothesized that nitrogen compounds might exhibit a similar trend. Given that three naphthenic rings have the same DBE as a single aromatic ring, nitrogen compounds with high carbon numbers may have shorter alkyl chains and/or less possibility of substitution near the nitrogen atom than those with medium carbon numbers. As a result, at least some nitrogen compounds with high carbon numbers may have less steric hindrance from alkyl chains than those with medium carbon numbers. Although there was no direct evidence, as shown in Fig. 11, we observed that as the HDN levels increased, the weighted arithmetic mean DBEs of basic and neutral nitrogen compounds with fixed carbon numbers first decreased and then stabilized. Additionally, despite the nitrogen compounds with higher carbon numbers having a higher DBE, the shift values of DBE at the initial stage compared to the feed decreased with increasing carbon numbers for both basic and neutral nitrogen compounds, which is consistent with previous research (Mikhaylova et al., 2022). Therefore, it is likely that high-carbon nitrogen compounds possess fewer aromatic rings compared to medium-carbon ones. Otherwise, given their greater reactivity, the high-carbon nitrogen compounds would be expected to exhibit higher DBE shift values than the medium-carbon compounds.

3.6. Molecular structures of the most refractory or abundant basic and neutral nitrogen compounds

After hydrotreatment, the molecular structures of the most recalcitrant or abundant basic and neutral nitrogen compounds can be inferred by examining the impact of DBE and carbon number on their reactivity. Fig. 4 shows that basic nitrogen compounds with a DBE of 8 and a carbon number between 23 and 33 were the most

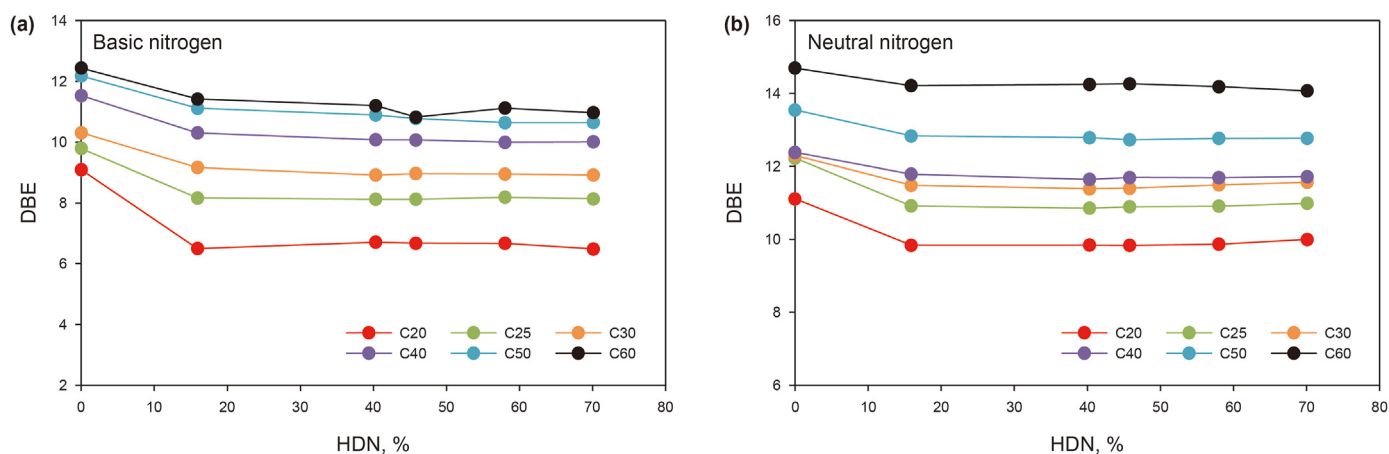


Fig. 11. Plots of the weighted arithmetic mean DBE of (a) basic nitrogen compounds and (b) neutral nitrogen compounds at fixed carbon numbers as a function of HDN ratio.

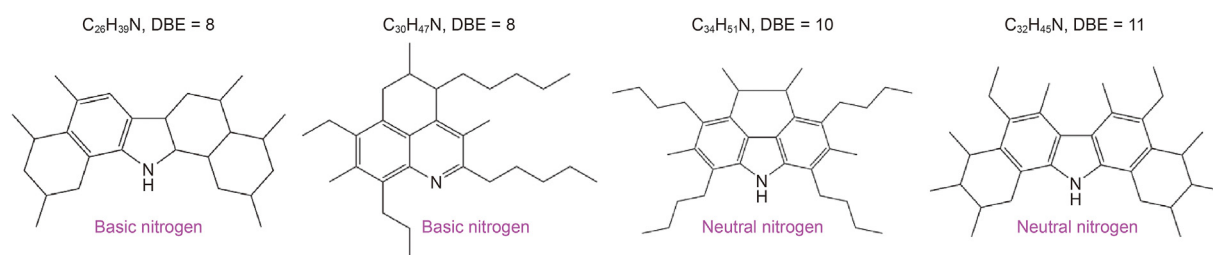


Fig. 12. Proposed molecular structures of the most refractory or abundant basic and neutral nitrogen compounds during the RHT process.

abundant. Meanwhile, neutral nitrogen compounds with DBEs of 10–11 and carbon numbers ranging from 28 to 39 were the most resistant. According to the discussions in Sections 3.3 and 3.4, the skeletons of the remaining basic nitrogen compounds with a DBE of 8 may consist primarily of three types: (1) those that had a DBE of 8 initially, (2) those that were transformed from basic nitrogen compounds with DBEs of 10, 12, or higher, and (3) those that were derived from neutral nitrogen compounds with DBEs of 11, 13, or higher. Regarding the most stubborn neutral nitrogen compounds, the skeletons of those that remain with a DBE of 10 may consist mainly of two types: (1) those that had a DBE of 10 initially, and (2) those that were transformed from compounds with a DBE of 12, or higher. The neutral nitrogen compounds with a DBE of 11 may include skeletons that originally had a DBE of 11, as well as those that were converted from DBEs of 13, 15, or higher. Concerning the carbon number, it has been reported that alkyl substitutions next to the nitrogen atom may display lower reactivity due to increased diffusion resistance (Le Maître et al., 2020). As a result, nitrogen compounds without a DBE shift may contain alkyl substitutions adjacent to the nitrogen atom, while those converted from higher DBEs may have low steric hindrance. Several molecular structures have been proposed for the refractory or abundant basic and neutral nitrogen compounds, as shown in Fig. 12. These compounds are believed to contain multiple naphthenic rings or long side chains near the nitrogen atom, in agreement with previous studies (Le Maître et al., 2020; Li et al., 2024).

4. Conclusions

During the RHT process, the proportion of basic nitrogen initially increased and then decreased as the HDN ratio increased. This phenomenon can be attributed, at least in part, to converting neutral nitrogen compounds into basic ones. Furthermore, the

refractory neutral nitrogen compounds were carbazoles, likely due to their low aromaticity and high steric hindrance. In contrast, the most abundant basic nitrogen compounds were quinolines. Through detailed analysis of the evolution of DBE, we revealed the intricate reaction mechanisms of benzocarbazoles and dibenzocarbazoles in residual oil, highlighting the crucial role of quinolines as key intermediates in the removal process of these compounds. Interestingly, nitrogen compounds with both low and high carbon numbers (for a given DBE) exhibited higher reactivity than those with medium carbon numbers. Consequently, the most refractory neutral nitrogen compounds were those with DBEs of 10–11 and carbon numbers between 28 and 39, while the most abundant basic nitrogen compounds were those with a DBE of 8 and carbon numbers between 23 and 33. The molecular structures of these compounds could be classified into two primary categories: those featuring multiple naphthenic-aromatic rings and those possessing long side chains proximate to the nitrogen atom. This comprehensive understanding provides a deeper insight into the HDN process, ultimately aiding in the rational design of RHT catalysts and process development. Nevertheless, further studies are suggested to investigate the molecular structural characteristics of nitrogen compounds with the same DBE but different carbon numbers and to develop a molecular-level HDN kinetic model.

CRediT authorship contribution statement

Zhong-Huo Deng: Writing – original draft, Methodology, Conceptualization. **Si-Yang Guo:** Methodology, Investigation. **Xin-Peng Nie:** Methodology, Investigation. **Xin-Heng Cai:** Formal analysis, Data curation. **Yan-Zi Jia:** Investigation. **Wei Han:** Writing – review & editing. **Li-Shun Dai:** Supervision, Resources.

Declaration of competing interest

The authors declare that they have no known competing financial interests or personal relationships that could have appeared to influence the work reported in this paper.

Acknowledgment

The authors gratefully acknowledge the financial support from the National Key Research and Development Program of China (2021YFA1501204) and the project of SINOPEC RIPP Co. Ltd (PR20230230).

Appendix A. Supplementary data

Supplementary data to this article can be found online at <https://doi.org/10.1016/j.petsci.2025.02.015>.

References

- Abu, I.I., Smith, K.J., 2007. Hydrodenitrogenation of carbazole over a series of bulk Ni/MoP catalysts. *Catal. Today* 125, 248–255. <https://doi.org/10.1016/j.cattod.2007.02.035>.
- Adamski, G., Dyrek, K., Kotarba, A., Sojka, Z., Sayag, C., Djéga-Mariadassou, G., 2004. Kinetic model of indole HDN over molybdenum carbide: influence of potassium on early and late denitrogenation pathways. *Catal. Today* 90, 115–119. <https://doi.org/10.1016/j.cattod.2004.04.015>.
- Al-Hajji, A.A., Muller, H., Koseoglu, O.R., 2008. Characterization of nitrogen and sulfur compounds in hydrocracking feedstocks by fourier transform ion cyclotron mass spectrometry. *Oil & Gas Science and Technology - Revue de l'IFP* 63, 115–128. <https://doi.org/10.2516/ogst.2008001>.
- Ancheyta, J., Rana, M.S., Furimsky, E., 2005. Hydroprocessing of heavy petroleum feeds: tutorial. *Catal. Today* 109, 3–15. <https://doi.org/10.1016/j.cattod.2005.08.025>.
- Ávila, B.M.F., Vaz, B.G., Pereira, R., Gomes, A.O., Pereira, R.C.L., Corilo, Y.E., Simas, R.C., Nascimento, H.D.L., Eberlin, M.N., Azevedo, D.A., 2012. Comprehensive chemical composition of gas oil cuts using two-dimensional gas chromatography with time-of-flight mass spectrometry and electrospray ionization coupled to fourier transform ion cyclotron resonance mass spectrometry. *Energy Fuels* 26, 5069–5079. <https://doi.org/10.1021/ef300631e>.
- Bachrach, M., Marks, T.J., Notestein, J.M., 2016. Understanding the hydrodenitrogenation of heteroaromatics on a molecular level. *ACS Catal.* 6, 1455–1476. <https://doi.org/10.1021/acscatal.5b02286>.
- Bello, S.S., Wang, C., Zhang, M., Gao, H., Han, Z., Shi, L., Su, F., Xu, G., 2021. A review on the reaction mechanism of hydrodesulfurization and hydrodenitrogenation in heavy oil upgrading. *Energy & Fuels* 35 (14), 10998–11016. <https://doi.org/10.1021/acs.energyfuels.1c01015>.
- Celis-Cornejo, C.M., Pérez-Martínez, D.J., Orrego-Ruiz, J.A., Baldovino-Medrano, V.G., 2018. Identification of refractory weakly basic nitrogen compounds in a deeply hydrotreated vacuum gas oil and assessment of the effect of some representative species over the performance of a Ni-MoS₂/Y-Zeolite-Alumina catalyst in phenanthrene hydrocracking. *Energy Fuels* 32, 8715–8726. <https://doi.org/10.1021/acs.energyfuels.8b02045>.
- Chacón-Patiño, M.L., Blanco-Tirado, C., Orrego-Ruiz, J.A., Gómez-Escudero, A., Combariza, M.Y., 2015. Tracing the compositional changes of asphaltenes after hydroconversion and thermal cracking processes by high-resolution mass spectrometry. *Energy Fuels* 29, 6330–6341. <https://doi.org/10.1021/acs.energyfuels.5b01510>.
- Cho, Y., Kim, Y.H., Kim, S., 2011. Planar limit-assisted structural interpretation of saturates/aromatics/resins/asphaltene fractionated crude oil compounds observed by fourier transform ion cyclotron resonance mass spectrometry. *Anal. Chem.* 83, 6068–6073. <https://doi.org/10.1021/ac2011685>.
- Cho, Y., Na, J.G., Nho, N.S., Kim, Sunghong, Kim, Sunghwan, 2012. Application of saturates, aromatics, resins, and asphaltene crude oil fractionation for detailed chemical characterization of heavy crude oils by fourier transform ion cyclotron resonance mass spectrometry equipped with atmospheric pressure photoionization. *Energy Fuels* 26, 2558–2565. <https://doi.org/10.1021/ef201312m>.
- Deng, Z., Dai, L., Han, W., Cai, X., Nie, X., Fang, Q., Nie, H., 2022. Towards a deep understanding of the evolution and molecular structures of refractory sulfur compounds during deep residue hydrotreating process. *Fuel Process. Technol.* 231, 107235. <https://doi.org/10.1016/j.fuproc.2022.107235>.
- Furimsky, E., 1999. Deactivation of hydroprocessing catalysts. *Catal. Today* 52, 381–495. [https://doi.org/10.1016/S0920-5861\(99\)00096-6](https://doi.org/10.1016/S0920-5861(99)00096-6).
- Furimsky, E., Massoth, F.E., 2005. Hydrodenitrogenation of petroleum. *Catal. Rev. Sci. Eng.* 47, 297–489. <https://doi.org/10.1081/CR-200057492>.
- Guillemant, J., Albrieux, F., De Oliveira, L.P., Lacoue-Nègre, M., Duponchel, L., Joly, J.F., 2019. Insights from nitrogen compounds in gas oils highlighted by high-resolution fourier transform mass spectrometry. *Anal. Chem.* 91, 12644–12652. <https://doi.org/10.1021/acs.analchem.9b01702>.
- Guillemant, J., Berlioz-Barbier, A., De Oliveira, L.P., Albrieux, F., Lacoue-Nègre, M., Duponchel, L., Joly, J.F., 2020. Exploration of the reactivity of heteroatomic compounds contained in vacuum gas oils during hydrotreatment using fourier transform ion cyclotron resonance mass spectrometry. *Energy Fuels* 34, 10752–10761. <https://doi.org/10.1021/acs.energyfuels.0c01760>.
- Ho, T.C., Katritzky, A.R., Cato, S.J., 1992. Effect of nitrogen compounds on cracking catalysts. *Ind. Eng. Chem. Res.* 31, 1589–1597. <https://doi.org/10.1021/ie00007a002>.
- Lai, T., Mao, Y., Wang, W., Wang, X., Wang, N., Liu, Z., 2020. Characterization of basic nitrogen compounds isolated with FeCl₃ in vacuum gas oil and its hydrotreated product. *Fuel* 262, 116523. <https://doi.org/10.1016/j.fuel.2019.116523>.
- Laredo, G.C., Montesinos, A., De Los Reyes, J.A., 2004. Inhibition effects observed between dibenzothiophene and carbazole during the hydrotreating process. *Appl. Catal. Gen.* 265, 171–183. <https://doi.org/10.1016/j.apcata.2004.01.013>.
- Le Maître, J., Hubert-Roux, M., Paupy, B., Marceau, S., Rüger, C.P., Afonso, C., Giusti, P., 2019. Structural analysis of heavy oil fractions after hydrodenitrogenation by high-resolution tandem mass spectrometry and ion mobility spectrometry. *Faraday Discuss* 218, 417–430. <https://doi.org/10.1039/c8fd00239h>.
- Le Maître, J., Paupy, B., Hubert-Roux, M., Marceau, S., Rüger, C., Afonso, C., Giusti, P., 2020. Structural analysis of neutral nitrogen compounds refractory to the hydrodenitrogenation process of heavy oil fractions by high-resolution tandem mass spectrometry and ion mobility-mass spectrometry. *Energy Fuels* 34, 9328–9338. <https://doi.org/10.1021/acs.energyfuels.0c01160>.
- Li, S., Mo, C., Cai, X., Zhang, Q., Long, J., Zhang, L., Qian, K., Cai, Q., Wang, W., 2024. Enrichment of nitrogen compounds in heavy oils by complexation with ZrCl₄ and detailed characterization using FT-ICR MS and ion mobility spectrometry. *Sep. Purif. Technol.* 336, 126132. <https://doi.org/10.1016/j.seppur.2023.126132>.
- Li, Y.E., Guan, Y.M., Liu, M., Yuan, S.H., Zhang, C., Song, Y.Y., 2021. Transformation of basic and non-basic nitrogen compounds during heavy oil hydrotreating on two typical catalyst gradations. *Energy Fuels* 35, 2826–2837. <https://doi.org/10.1021/acs.energyfuels.0c03028>.
- Li, Z., Wang, G., Gao, J., 2019. Effect of retarding components on heavy oil catalytic cracking and their corresponding countermeasures. *Energy Fuels* 33, 10833–10843. <https://doi.org/10.1021/acs.energyfuels.9b02728>.
- Liu, L., Song, C., Tian, S., Zhang, Q., Cai, X., Liu, Y., Liu, Z., Wang, W., 2019. Structural characterization of sulfur-containing aromatic compounds in heavy oils by FT-ICR mass spectrometry with a narrow isolation window. *Fuel* 240, 40–48. <https://doi.org/10.1016/j.fuel.2018.11.130>.
- Liu, M., Zhang, L., Zhao, S., Zhao, D., 2016. Transformation of nitrogen compounds through hydrotreatment of Saudi Arabia atmospheric residue and supercritical fluid extraction subfractions. *Energy Fuels* 30, 740–747. <https://doi.org/10.1021/acs.energyfuels.5b02158>.
- Liu, M., Zhang, L.Z., Zhang, C., Yuan, S.H., Zhao, D.Z., Duan, L.H., 2018. Transformation of nitrogen-containing compounds in atmospheric residue by hydrotreating. *Kor. J. Chem. Eng.* 35, 375–382. <https://doi.org/10.1007/s11814-017-0305-9>.
- Liu, M., Zhao, D.Z., Zhang, L.Z., Zhao, S.Q., 2017. Stepwise structural characterization of hydrocarbon compounds and polar components during atmospheric residue hydrotreatment. *Fuel Process. Technol.* 158, 238–246. <https://doi.org/10.1016/j.fuproc.2017.01.007>.
- Marafi, A., Albazzaz, H., Rana, M.S., 2019. Hydroprocessing of heavy residual oil: opportunities and challenges. *Catal. Today* 329, 125–134. <https://doi.org/10.1016/j.cattod.2018.10.067>.
- Massoth, F.E., Kim, S.C., 2003. Kinetics of the HDN of quinoline under vapor-phase conditions. *Ind. Eng. Chem. Res.* 42, 1011–1022. <https://doi.org/10.1021/ie020390t>.
- Mierau, J.M.J.B., Zhang, N., Tan, X., Scherer, A., Stryker, J.M., Tykwinski, R.R., Gray, M.R., 2015. Catalytic hydrodenitrogenation of asphaltene model compounds. *Energy Fuels* 29, 6724–6733. <https://doi.org/10.1021/acs.energyfuels.5b01853>.
- Mikhaylova, P., de Oliveira, L.P., Merdriagnac, I., Berlioz-Barbier, A., Nemri, M., Giusti, P., Pirngruber, G.D., 2022. Molecular analysis of nitrogen-containing compounds in vacuum gas oils hydrodenitrogenation by (ESI+/-)-FTICR-MS. *Fuel* 323, 124302. <https://doi.org/10.1016/j.fuel.2022.124302>.
- Nagai, M., Masunaga, T., 1988. Hydrodenitrogenation of a mixture of basic and non-basic polynuclear aromatic nitrogen compounds. *Fuel* 67, 771–774. [https://doi.org/10.1016/0016-2361\(88\)90148-2](https://doi.org/10.1016/0016-2361(88)90148-2).
- Nguyen, M.T., Pirngruber, G.D., Chainet, F., Albrieux, F., Tayakout-Fayolle, M., Geantet, C., 2019. Molecular-level insights into coker/straight-run gas oil hydrodenitrogenation by fourier transform ion cyclotron resonance mass spectrometry. *Energy Fuels* 33, 3034–3046. <https://doi.org/10.1021/acs.energyfuels.8b04432>.
- Nguyen, M.T., Tayakout-Fayolle, M., Chainet, F., Pirngruber, G.D., Geantet, C., 2017. Use of kinetic modeling for investigating support acidity effects of NiMo sulfide catalysts on quinoline hydrodenitrogenation. *Appl. Catal. Gen.* 530, 132–144. <https://doi.org/10.1016/j.apcata.2016.11.015>.
- Ni, H., Xu, C., Wang, R., Guo, X., Long, Y., Ma, C., Yan, L., Liu, X., Shi, Q., 2018. Composition and transformation of sulfur-, oxygen-, and nitrogen-containing compounds in the hydrotreating process of a low-temperature coal tar. *Energy Fuels* 32, 3077–3084. <https://doi.org/10.1021/acs.energyfuels.7b03659>.
- Ovalles, C., Rogel, E., Lopez, J., Pradhan, A., Moir, M., 2013. Predicting reactivity of feedstocks to resid hydroprocessing using asphaltene characteristics. *Energy Fuels* 27, 6552–6559. <https://doi.org/10.1021/ef401471v>.
- Pei, L., Li, D., Liu, X., Cui, W., Shao, R., Xue, F., Li, W., 2017. Investigation on asphaltene structures during low temperature coal tar hydrotreatment under various reaction temperatures. *Energy Fuels* 31, 4705–4713. <https://doi.org/10.1021/>

- acs.energyfuels.6b03180.
- Prado, G.H.C., Rao, Y., De Klerk, A., 2017. Nitrogen removal from oil: a review. *Energy Fuels* 31, 14–36. <https://doi.org/10.1021/acs.energyfuels.6b02779>.
- Prins, R., Egorova, M., Röthlisberger, A., Zhao, Y., Sivasankar, N., Kukula, P., 2006. Mechanisms of hydrodesulfurization and hydrodenitrogenation. *Catal. Today* 111, 84–93. <https://doi.org/10.1016/j.cattod.2005.10.008>.
- Prins, R., Jian, M., Flechsenhar, M., 1997. Mechanism and kinetics of hydrodenitrogenation. *Polyhedron* 16, 3235–3246. [https://doi.org/10.1016/S0277-5387\(97\)00111-3](https://doi.org/10.1016/S0277-5387(97)00111-3).
- Prins, R., Zhao, Y., Sivasankar, N., Kukula, P., 2005. Mechanism of CN bond breaking in hydrodenitrogenation. *J. Catal.* 234, 509–512. <https://doi.org/10.1016/j.jcat.2005.06.034>.
- Purcell, J.M., Merdrignac, I., Rodgers, R.P., Marshall, A.G., Gauthier, T., Guibard, I., 2010. Stepwise structural characterization of asphaltenes during deep hydroconversion processes determined by atmospheric pressure photoionization (APPI) fourier transform ion cyclotron resonance (FT-ICR) mass spectrometry. *Energy Fuels* 24, 2257–2265. <https://doi.org/10.1021/ef900897a>.
- Purcell, J.M., Rodgers, R.P., Hendrickson, C.L., Marshall, A.G., 2007. Speciation of nitrogen containing aromatics by atmospheric pressure photoionization or electrospray ionization fourier transform ion cyclotron resonance mass spectrometry. *J. Am. Soc. Mass Spectrom.* 18, 1265–1273. <https://doi.org/10.1016/j.jasms.2007.03.030>.
- Rogel, E., Witt, M., 2017. Asphaltene characterization during hydroprocessing by ultrahigh-resolution fourier transform ion cyclotron resonance mass spectrometry. *Energy Fuels* 31, 3409–3416. <https://doi.org/10.1021/acs.energyfuels.6b02363>.
- Szymańska, A., Lewandowski, M., Sayag, C., Djéga-Mariadassou, G., 2003. Kinetic study of the hydrodenitrogenation of carbazole over bulk molybdenum carbide. *J. Catal.* 218, 24–31. [https://doi.org/10.1016/S0021-9517\(03\)00072-1](https://doi.org/10.1016/S0021-9517(03)00072-1).
- Zhang, T., Zhang, L., Zhou, Y., Wei, Q., Chung, K.H., Zhao, S., Xu, C., Shi, Q., 2013. Transformation of nitrogen compounds in deasphalted oil hydrotreating: characterized by electrospray ionization fourier transform-ion cyclotron resonance mass spectrometry. *Energy Fuels* 27, 2952–2959. <https://doi.org/10.1021/ef400154u>.
- Zhang, Y., Chen, X., Zhang, L., Shi, Q., Zhao, S., Xu, C., 2020. Specification of the nitrogen functional group in a hydrotreated petroleum molecule using hydrogen/deuterium exchange electrospray ionization high-resolution mass spectrometry. *Analyst* 145, 4442–4451. <https://doi.org/10.1039/d0an00772b>.
- Zhang, Y., Zhang, L., Xu, Z., Zhang, N., Chung, K.H., Zhao, S., Xu, C., Shi, Q., 2014. Molecular characterization of vacuum resid and its fractions by Fourier transform ion cyclotron resonance mass spectrometry with various ionization techniques. *Energy Fuels* 28, 7448–7456. <https://doi.org/10.1021/ef502162b>.
- Zhao, J., Liu, T., Han, W., Ren, L., Zhang, L., Dai, L., Li, D., 2021. An insight into the molecular structure of sulfur compounds and their reactivity during residual oil hydroprocessing. *Fuel* 283, 119334. <https://doi.org/10.1016/j.fuel.2020.119334>.
- Zhu, Y., Yang, T., Li, G., Guo, Y., Yang, C., Teng, H., Xu, M., Du, C., Wang, C., Li, D., 2022. Insight into asphaltene transformation during coal tar hydrotreatment by conventional analysis and high-resolution Fourier transform mass spectrometry coupled with collision-induced dissociation technology. *J. Energy Inst.* 103, 17–32. <https://doi.org/10.1016/j.joei.2022.05.007>.